

# PREDICTION OF LOW-FREQUENCY VIBRATION TRANSMISSION THROUGH AN AUTOMOTIVE DOOR MOUNT SYSTEM USING THE FINITE ELEMENT METHOD

DA DESAI, RC AYLWARD, CJ SMITH AND J ERASMUS

## ABSTRACT

The phenomenon of automotive door panel vibration is complex, because it comprises the simultaneous interaction of many competing factors. Numerical simulation of such behaviour is not simplistic and is challenging at both the scientific and technical levels. Anecdotal evidence suggests that, until now, the characterisation of door panel vibration in terms of its door mount system has not yet been contemplated. This paper describes a numerical model and its application to a case study to investigate the vibrational behaviour of a door panel in terms of its door mount system. Results of the numerical model are compared with those obtained from physical measurements and are found to be satisfactory.

**Keywords:** Fluid-structure interaction; automotive door mounts; door panel vibration; numerical modelling; finite element method.

## 1. INTRODUCTION

In recent years, the complexity of the automotive design process has become greater on account of regulatory actions arising from the social and environmental consequences of millions of motor vehicles operating on our highways. As a result, there has been considerable interest in investigating methodologies for reducing vibration amplitudes in transportation systems. Consequently, a relative contribution of secondary-level vibrational sources, such as structural surfaces and components, has become the limiting factor in the quest for the improvement of passenger comfort. Market research indicates that door mounts are designed based on strength only and selection procedures for door mount systems are frequently of an anecdotal or historical nature. It was felt that these approaches may lead to conservative designs. Because of the challenges faced by automotive manufacturers in terms of passenger comfort, it has now become imperative to select door mounts that satisfy both strength and vibration criteria.

Most internal noise is associated with the dynamic behaviour of the vehicle body structure at frequencies below 400 Hz (Morrey & Barr, 1996). While the vibration amplitudes of typical door panels are small and might not be visualised most of the time, they can cause significant noise, which we definitely hear and therefore cannot ignore (Irato et al., 1995). Although individual components such as door panels may behave satisfactorily in isolation, their interaction with other components can cause serious problems.

Though there have been extensive studies on sound radiation from vibrating plates with classical boundary conditions, no comparable efforts have been made to determine the contribution of accompanying structural components with non-classical boundary conditions, such as automotive door mounts.

Furthermore, the morphology of complex, built-up, fluid-mechanical structures possessing multi-body dynamics, generally exhibit important degrees of uncertainty and variability due to the presence of damping, varying stiffness, joints and joint position. According to Desmet and Sas (1996), a limited number of publications addressing the damping phenomena within fluid-structure interaction systems have been documented and an even smaller number of experimental verifications have been undertaken to confirm theoretical approaches. A possible reason could be that many researchers use hypothetical damping ratios for the sake of completeness, thereby making experimental validation impossible. In addition, Marburg (2004) reports that many of these studies have used classical support conditions or neglected the supports altogether, whilst a few used unrealistic rigid supports.

Without a mechanistic understanding of how such uncertainties and mechanisms affect vibrational performance, extrapolating past empirical data to new conditions could involve unknown factors that may produce unreliable results, high costs and increased development lead times. Therefore, the simultaneous interaction of the above uncertainties, complexities and competing factors require computer-based tools, because such systems are too complex and time consuming to be analysed analytically. The development of a predictive model is therefore an effective and sensible approach.

However, there are many difficult modelling issues that pose tough challenges at both the scientific and the technical levels in simulating the dynamics of such systems. Some of the complexities are introduced by the dynamics of structural joints and multi-bodies, the interaction between structural panels and interior acoustics, the damping characteristics, the intricate shape of the passenger cabin and non-linear dynamic behaviours.

For the numerical solution of the vibration transmission through the door mount system at a moderate computational cost, a model is developed based on a fully-coupled modal superposition scheme employing the ABAQUS® finite element code. Factors such as hyperelasticity, contact, friction, bolt loads and energy dissipation are considered. This paper outlines the numerical modelling procedure and framework used to simulate the vibrational behaviour of a simplified automotive door panel in terms of its mount system. To test the validity of the proposed model, an experimental campaign was undertaken, the results of which were found to be satisfactory.

## 2. DESCRIPTION AND GEOMETRY OF THE PHYSICAL MODEL

In order to minimise computational efforts and costs, a simplified car body of approximately one-third scale is used, stripped of its internal trimming, but with its door mounts, door seal, latch and striker mechanism remaining as in production. In the context of this study, vibration is transferred from the vehicle body to the door panels through the door mounts and the latch and striker mechanism. Therefore, the system under study consists essentially of a vehicle's front right-hand door panel with its respective upper and lower door mount assemblies, a door seal and a vehicle body structure constituting an enclosed passenger cabin. The door is articulated by means of the door mount assemblies connected to the A-pillar and door, respectively. A stiff vehicle structure is created in order to maintain approximate relative occurrence of acoustic and structural modes over the low-frequency domain on par with a typical full-size real vehicle structure. The test structure is constructed from both 25 mm square and 100 mm × 50 mm mild steel tubing (A-pillar); clad by 3 mm thick mild steel plates. The passenger cabin is acoustically sealed by means of a door seal at the front right-hand door. The test structure under consideration is shown in Fig. 1, the components of which are representative of systems used in domestic passenger vehicles.

Table 1 summarises the description of the test model. The mount separating distances are relative to the upper and lower door mounts, while the latch position is relative to the door's central horizontal axis (x-axis).

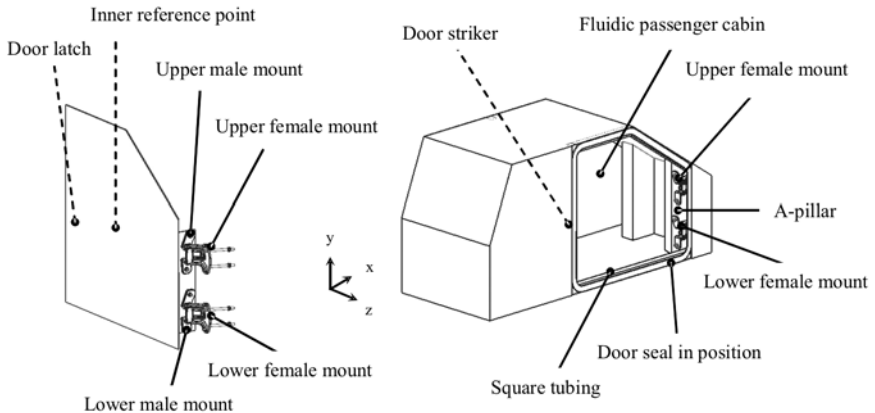


Figure 1: Simplified vehicle with actual door mount system

Table 1: Description of test model

Description			
Fixation method at A-pillar: door panel	Number of mounts	Mount separation distance (mm)	Latch position
bolt: bolt	2	148	middle

### 3. MATHEMATICAL MODELS

#### 3.1 Hyperelastic door seal model

In this work, the popular olefinic, EPDM sponge-dense, elastomeric door seal is used. The constitutive behaviour of this material is assumed to be purely elastic and its compressibility effects are representable by the finite deformation hyperelastic model recommended by Morman (1998). This model is based on the assumption that the material is isotropic relative to its undeformed and unstressed configuration and that its elastic properties are characterised by a strain-energy function. Due to the high compressibility of EPDM sponge rubber, classical isotropic, elastomeric and low compressibility theories, such as the Mooney-Rivlin form, are not appropriate for the case studied in this work.

Hence, special non-linear considerations are required to model the door seal. Research indicates that such materials may be characterised by either the hyperelastic constitutive law proposed by Blatz and Ko, as cited by Morman (1998) and Wagner et al. (1997), which accounts for the high compressibility of the sponge rubber and the non-linear stress-strain relationship, or by the Marlow strain potential model. However, experience has shown that, whenever test data are available, the Marlow strain potential model is preferred for the characterisation of hyperelastic material behaviour and is therefore used in this work. The Marlow model assumes that the strain energy potential is independent of the second deviatoric strain invariant and is defined by providing experimental test data to describe the deviatoric behaviour. The code constructs a strain energy potential that reproduces the test data exactly and has reasonable behaviour in other deformation modes. The Poisson parameter determines the volumetric response of the door seal throughout its deformation process. The Marlow strain energy potential may be expressed in the form

$$U = U_{dev}(\bar{I}_1) + U_{vol}(J_{el}) \quad (1)$$

where  $\bar{I}_1$  represents the first deviatoric strain invariant,  $U$  is the strain energy per unit of reference volume with  $U_{dev}$  as its deviatoric part and  $U_{vol}$  as its volumetric part.  $J_{el}$  represents the elastic volume ratio. The deviatoric part

of the potential is defined by providing biaxial test data depicted in Table 2. In order to include the effects of compressibility of the door seal, the volumetric part of Eq. (1) is defined by prescribing a Poisson's ratio value  $\nu_o = 0.4$ . A 91% seal compression, similar to that used by Stenti, Moens and Desmet (2004), which represents the door seal compression level of a typical sedan, was used in this study.

Table 2: Biaxial test data for EPDM sponge rubber in compression

Nominal stress (Pa)	Nominal strain
$2.150 \times 10^6$	-0.357
$1.880 \times 10^6$	-0.324
$1.610 \times 10^6$	-0.286
$1.340 \times 10^6$	-0.242
$1.070 \times 10^6$	-0.190
$8.057 \times 10^5$	-0.139
$5.371 \times 10^5$	-0.090
$2.686 \times 10^5$	-0.043
0.000	-0.000

### 3.2 Energy dissipation

In general, three modes of damping are dominant in this study, namely hysteretic, viscoelastic and Coulomb damping, the latter due to slippage in the bolted mount connections. However, according to Allemang and Brown (1996), it is a well-established fact that determining the damping factors required for these damping modes in complex structures is very difficult due to the rather extensive experimental data that should be acquired. Therefore, an approximate spectral model is suggested and employed in this work.

With spectral damping approaches, experimental observations of the vibratory response of structures are used to assign a fraction of critical damping as a function of frequency, as cited by Cook, Malkus and Plesha (1989). A popular spectral damping scheme recommended by many researchers, such as Inman (1994), to approximate the equivalent resultant damping phenomena, as defined by Cook, Malkus and Plesha (1989), is the modal damping scheme, where the damping in each eigenmode can be given as a fraction of the critical damping for that mode. Modal damping introduces an energy dissipation term of the form

$$\delta W_{diss} = 2 \zeta_i \omega_i \dot{u}_i \quad (2)$$

where  $\zeta_i$  is the  $i^{\text{th}}$  modal damping ratio,  $\omega_i$  is the  $i^{\text{th}}$  natural frequency and  $\dot{u}_i$  is the velocity.

### 3.3 The friction model

Interface modelling is employed to represent surface interactions that occur at the door latch and striker mechanism and between bolt faces and their respective mating surfaces in cases where bolted mount connections are employed. The mount base contact surfaces on both male and female mounts, as well as the bolt and nut contact faces, are considered, for such modelling improves the accuracy of the predictive model. In order to model any potential slip in the bolts, the tangential surface behaviour is described in terms of the isotropic Coulomb friction model, based on the simplified model proposed by Wriggers, Vu van T and Stein (1990), with a limit on the allowable shear stress. Thus, the stiffness of structural connections, such as bolted door mounts, is determined by contact deformations between the connected surfaces and, therefore, by contact pressures. The contact pressures themselves are generated by tightening (pre-loading) the bolts, thus creating a joint-tightening force between the bolt heads and the thread. Because the dynamic response is sought, the slip coefficient of friction values are used, where applicable.

The shear stress limit model allows for the introduction of a maximum value of shear stress that can be carried by the interface before the surfaces begin to slide. The coefficient of friction model may be represented directly as

$$\mu = \mu(\dot{\gamma}_{eq}, p) \quad (3)$$

where  $\dot{\gamma}_{eq}$  is the equivalent slip rate and  $p$  is the contact pressure. The Coulomb friction model defines this critical shear stress  $\tau_{critical}$ , at which sliding of the surfaces starts as a fraction of the contact pressure between the surfaces ( $\tau_{critical} = \mu p$ ). Once the maximum shear stress limit, which is defined for all frictional contact surfaces involved, is exceeded, slipping of the relevant surfaces occur.

## 4. MATHEMATICAL FORMULATION

### 4.1 Governing equations

The vehicle structure and its respective components are modelled as deformable bodies comprising flexible wall panels of mass  $M$  enclosing a fluidic cavity. The front right-hand door panel is supported on two elastic door mounts. The case under investigation is idealised as a damped, multi-degree-of-freedom system subjected to a structurally induced, excitation force. According to Zhang and Brown (1996) and Zienkiewicz and Taylor (2000), a fully-coupled fluid-structure interaction system can be represented in a finite element type discretisation matrix form by

$$\begin{bmatrix} M_s & 0 \\ A & M_f \end{bmatrix} \begin{Bmatrix} \ddot{u}_s \\ \ddot{p}_f \end{Bmatrix} + \begin{bmatrix} C_s & 0 \\ 0 & C_f \end{bmatrix} \begin{Bmatrix} \dot{u}_s \\ \dot{p}_f \end{Bmatrix} + \begin{bmatrix} K_s & -A^T \\ 0 & K_f \end{bmatrix} \begin{Bmatrix} u_s \\ p_f \end{Bmatrix} = \begin{Bmatrix} f_s \\ f_f \end{Bmatrix} \quad (4)$$

where  $M$ ,  $C$  and  $K$  are the mass, damping and stiffness matrices with the subscripts  $s$  and  $f$  representing the structure and fluid medium, respectively.

$\ddot{\mathbf{u}}_s$ ,  $\dot{\mathbf{u}}_s$  and  $\mathbf{u}_s$  represent the structural acceleration, velocity and displacement vectors, respectively at the nodes of the finite element model. The non-symmetric matrix  $A$  represents the coupling between the structure and the cavity and may be expressed as

$$\mathbf{A} = \rho \mathbf{K}_c \quad (5)$$

with  $K_c$  being the coupled stiffness matrix. The damping term may be represented as

$$\mathbf{C}_s = 2\zeta_\alpha \omega_\alpha \quad (6)$$

where  $\alpha$  represents the mode number.

## 4.2 Boundary conditions

The boundary of the fluidic medium (air) within the passenger cabin is divided into superficial sub-regions  $S$ , on which the following relevant conditions are imposed: On  $S$ , where the motion of the fluidic medium is directly coupled to the motion of the solid (fluid-structural boundary), the fluid and structural media have the same displacement normal to the boundary, but the tangential motions are uncoupled. Therefore, the fluidic and structural media have the same acceleration normal to the boundary, so that

$$\mathbf{n} \cdot \ddot{\mathbf{u}}^f = \mathbf{n} \cdot \ddot{\mathbf{u}}^m \quad (7)$$

where  $\mathbf{n}$  the vector  $\mathbf{n}$  represents the inward normal to the fluidic medium at the boundary and  $\ddot{\mathbf{u}}^m$  is the structural particle acceleration. The rigid shaker base plate, to which the vehicle structure is attached, is assigned a displacement boundary condition, for which all degrees-of-freedom are fixed in the numerical analysis by default. This is so, since the fixed kinematic boundary conditions in an eigenfrequency step (this step is necessary for computation of the mode-based solution as described in section 5) cannot be changed in the subsequent mode-based procedure, because the kinematic constraints are built into the eigenvectors. However, since the structure needs to be dynamically excited in the vertical direction and it is not possible to prescribe non-zero displacements directly to mimic the action of the electromagnetic shaker as boundary conditions in a mode-based dynamic procedure, the motion of nodes on the shaker is specified as secondary base motion using the "big mass" approach. The desired base motion is obtained by applying a point force to each degree-of-freedom in the modal superposition step.

## 5. NUMERICAL SOLUTION

For the numerical solution of the vibration transmitted through a door mount system, a model is developed using modal superposition procedures in order to minimise computational cost. The solution is obtained using a full harmonic analysis at 113 frequencies between 9.38 and 199.38 Hz. The governing equation of motion represented by Eq. (4) may be discretised by introducing interpolation functions in both the fluidic and structural mediums. In order to use the Galerkin method, mathematical manipulations and discretisations of relevant equations (not discussed in this work) are performed so that the variational fields become dimensionally consistent and can be chosen with the same interpolation. Thus, by subsequent Petrov-Galerkin substitution, we get

$$\begin{aligned}
 & -\delta \hat{p}^P \left\{ \left( \mathbf{M}_{f_r}^{PQ} + \mathbf{M}_{f_r}^{PQ} \right) \Delta \hat{p}^Q + \left( \mathbf{C}_{f_r}^{PQ} + \mathbf{C}_{f_r}^{PQ} \right) \Delta \hat{p}^Q + \left( \mathbf{K}_{f_r}^{PQ} + \mathbf{K}_{f_r}^{PQ} \right) \Delta p^Q \right\} \\
 & + \delta u^N \left\{ \mathbf{K}^{NM} \Delta u^M + \mathbf{M}^{NM} \Delta \ddot{u}^M + \left( \mathbf{C}_{(m)}^{NM} + \mathbf{C}_{(k)}^{NM} \right) \Delta \dot{u}^M + \left[ S_{f_r}^{QN} \right]^T \Delta p^Q - \Delta p^N \right\} = 0
 \end{aligned} \quad (8)$$

with

$$\mathbf{C}_f^{PQ} = \int_{V_f} \frac{r}{p_f^2 + \frac{r^2}{\omega^2}} \frac{\partial H^P}{\partial \mathbf{x}} \cdot \frac{\partial H^Q}{\partial \mathbf{x}} dV \quad (9)$$

$$\mathbf{K}_f^{PQ} = \int_{V_f} \frac{p_f}{p_f^2 + \frac{r^2}{\omega^2}} \frac{\partial H^P}{\partial \mathbf{x}} \cdot \frac{\partial H^Q}{\partial \mathbf{x}} dV \quad (10)$$

$$\mathbf{M}_f^{PQ} = \int_{V_f} \frac{1}{K_f} H^P H^Q dV \quad (11)$$

where  $\mathbf{C}_f^{PQ}$ ,  $\mathbf{K}_f^{PQ}$  and  $\mathbf{M}_f^{PQ}$  are the damping, stiffness and mass matrices of the fluidic elements, respectively with the superscripts  $P$ ,  $Q$  representing the pressure degrees-of-freedom in the fluid.  $\mathbf{C}_{f_r}^{PQ}$  and  $\mathbf{K}_{f_r}^{PQ}$  are the damping and stiffness matrices at the reactive fluidic boundary,  $r$  represents the volumetric drag and  $x$  is the spatial position of the fluid particle. Also, at the fluid-structural boundary,  $S_{fs}$ .

$$S_{fs}^{PM} = \int_{S_{fs}} H^P \mathbf{n} \cdot \mathbf{N}^M dS \quad (12)$$

where  $P$  and  $M$  are nodal variables. The structural stiffness is represented by

$$\mathbf{K}^{NM} = \int_V \left[ \frac{\partial \boldsymbol{\beta}^N}{\partial u^M} : \boldsymbol{\sigma}_o + \boldsymbol{\beta}^N : \mathbf{D} : \boldsymbol{\beta}^M \right] dV \quad (13)$$

where  $\beta$  is the strain interpolator and  $N$  and  $M$  represent the displacement degrees-of-freedom. Because of the fluid-structural coupling, the mass and stiffness matrices are non-symmetric. The superposition method briefly described in section 5.1 is used to solve Eq. (4) which is transformed to modal coordinates by first extracting a set of eigenvectors orthogonal with respect to the mass and stiffness matrix.

### 5.1 Mode-based steady-state dynamic analysis

In this work, the steady-state response of the case under investigation is based on the eigenmodes and eigenvalues of the system, where the mass and stiffness matrices and load vector of the physical door mount system is projected onto a set of eigenmodes resulting in diagonal systems in terms of modal amplitudes. The projection of the equations of motion of the system onto the  $\alpha$ th mode gives

$$\ddot{q}_\alpha + c_\alpha \dot{q}_\alpha + \omega_\alpha^2 q_\alpha = \frac{1}{m_\alpha} (f_{1\alpha} + i f_{2\alpha}) e^{i\omega t} \quad (14)$$

where  $q_\alpha$  represents the amplitude of mode  $\alpha$  (the  $\alpha^{\text{th}}$  “generalised coordinate”),  $c_\alpha$  is the damping associated with this mode defined by Eq. (6),  $\omega_\alpha$  is the undamped frequency of the mode,  $m_\alpha$  represents the generalised mass associated with the mode and  $(f_{1\alpha} + i f_{2\alpha}) e^{i\omega t}$  is the forcing function associated with this mode. The modal frequency response of the door panel displacement is expressed as

$$P(\bar{x}; \omega) = \sum_{\alpha=1}^N \phi_\alpha(\bar{x}) q_\alpha(\omega) \quad (15)$$

where  $P$  is the total response sought,  $\bar{x}$  is the spatial displacement,  $q_\alpha$  represents the amplitude of mode  $\alpha$  and  $\phi_\alpha$  is the eigenvector.

### 5.2 Eigen and residual modes

Since a very large number of eigenmodes are potentially excited on account of the temporal and spatial characteristics of the external excitation, it is necessary to extract and use many eigenmodes. However, due to computational cost (performance reasons), only a small subset of the total possible eigenmodes of the system is usually extracted, with the subset consisting of eigenmodes corresponding to eigenfrequencies that are close to the excitation frequency. This criterion alone does not guarantee that the system will be represented adequately by this set of eigenmodes; consequently, inaccuracies can occur in the modal dynamic solution. Therefore, the accuracy of the modal solution may suffer if too few higher frequency modes are used. Thus, a trade-off exists between accuracy and cost. To circumvent this and minimise the number of modes required for a sufficient degree of accuracy, the set of eigenmodes used in the projection and

superposition are augmented with residual modes. The residual mode capability can thus correct inaccuracies due to modal truncation, which are often prevalent in modal dynamic analyses, at a relatively lower cost than extracting additional eigenmodes arbitrarily.

In order to ensure that a sufficient number of eigenmodes are used, the literature suggests that the total effective mass in each orthogonal direction should be a large proportion (about 80%) of the mass of the model. By default, all the calculated eigenmodes and residual modes are used in the mode-based procedure. However, preliminary investigations based on a sensitivity analysis revealed that for large complicated systems, such as the one under investigation, a combination of residual modes and approximately 100 higher modes revealed the best compromise between accuracy (reasonable effective mass in all directions) and computational cost.

## **6. NUMERICAL MODELLING**

### **6.1 Contact interactions**

Deformable-to-deformable, small-sliding contact conditions are imposed on the model at all joints where relative sliding is permitted. The bottom of the bolt heads form contact-bearing surfaces with the top surfaces of the hinge flanges lying directly beneath them. All other respective mating (contact) surfaces are fully defined. Lateral slip of these mating components occurs if the critical frictional shear stress limit (described in section 3.3) is surpassed by lateral forces developed in the system. Contact condition definitions are not necessary between the bolt shanks and the holes in the door hinges, door and A-pillar because of the specified manufacturer's design clearance between them.

### **6.2 Mesh design**

A detailed, finite element model of the test structure, described in section 2, was created using a wide variety of appropriate finite elements and material properties in order to represent the behaviour of the various interacting bodies, adequately. Since material properties affect mesh parameters for wave problems and hence affect the accuracy of the solution, the discretisation protocol of the finite element method require at least six nodes per wavelength as cited by Lim (2000).

### **6.3 Loading conditions and step definitions**

The complexity of the system under investigation demands a multi-step approach comprising both non-linear simulation and linear perturbation sequences, to determine the steady-state response of the system when subjected to an excitation of 100 N applied vertically to the base of the model.

The finite element simulation progresses in seven steps as described in Fig. 2.

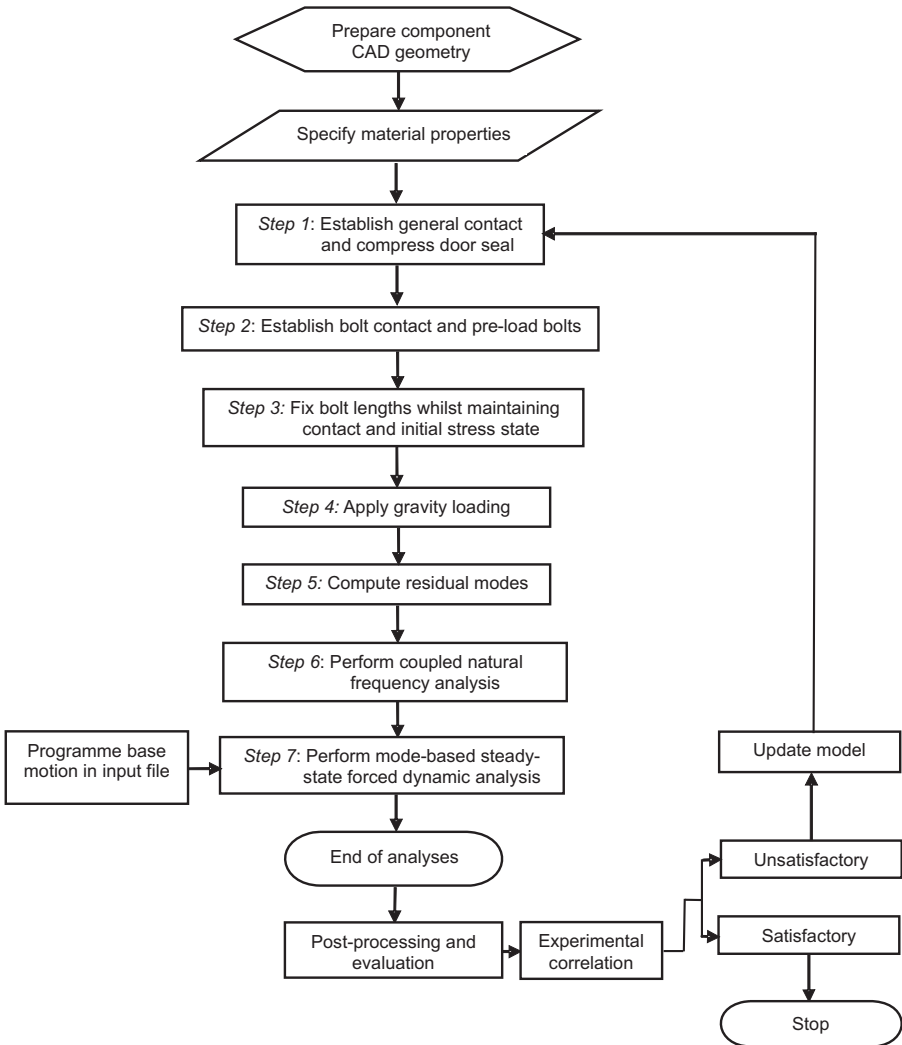


Figure 2: Solution strategy

## 7. RESULTS

### 7.1 Natural characteristics

Experimental damping ratios were recorded while exciting the vehicle under study on an electromagnetic shaker. The natural frequencies and modal damping factors computed for the first 11 modes are indicated in Table 3. The

first eigenvalue corresponds to a singular (constant pressure) acoustic mode. All eigenvectors are normalised with respect to displacement.

Table 3: Natural characteristics

Mode number										
Eigenfrequency (Hz)										
Modal damping factor										
1	2	3	4	5	6	7	8	9	10	11
96.3	97.2	125.3	140.2	142.5	160.1	163.9	171.3	183.5	189.5	191.3
0.052	0.051	0.049	0.041	0.042	0.048	0.049	0.036	0.039	0.038	0.039

## 7.2 Door panel vibration

The complete simulation converged at 2.95 hours of CPU time in 124 increments on a 2 GHz dual Xeon Pentium PC. An experimental campaign was undertaken to validate the predicted vibration signature. The predicted and measured displacement amplitude profiles at the inner reference point of the front right-hand door panel (see Fig. 1) in the y and z global directions are shown in Fig. 3. The comparisons indicate good correlation for such sensitive measurements, suggesting that the developed numerical model renders satisfactory and reliable results. The door displacement in the x global direction was negligible and therefore omitted.

Fig. 4 shows the peak resultant displacement field in metres of the complete vehicle in the structural motion amplitude at 124.7 Hz, which associates with mode 3. The dominant deflection zone involved is the roof panel. This area undergoes relatively large motion and is therefore most pronounced. The results indicate that the principal mode is a large displacement membrane-like deflection of the vehicle's roof panel with additional lower modes interacting with the structure to a lesser extent.

In order to facilitate easier identification of the peak displacement field and its corresponding frequency, a special code was written in the form of a PYTHON script that interacts directly with the output database. The code, currently non-existent in ABAQUS, interrogates the output database until the peak resultant displacement with its corresponding frequency is found. Fig. 5 shows the peak displacement field of the door panel, which occurs at 199.38 Hz.

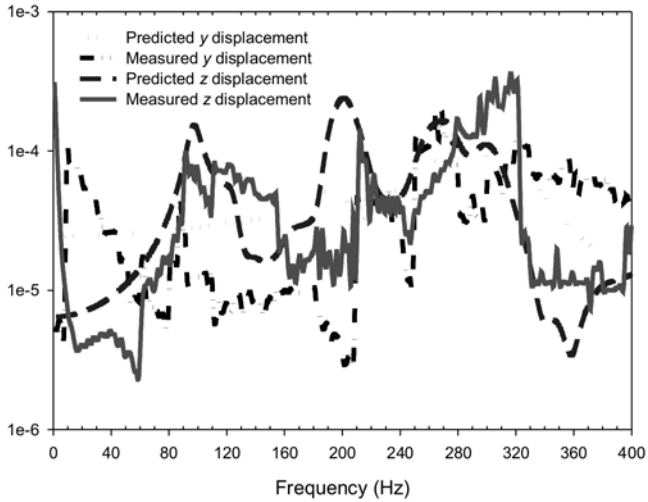


Figure 3: Comparison between predicted and measured door panel displacement signatures

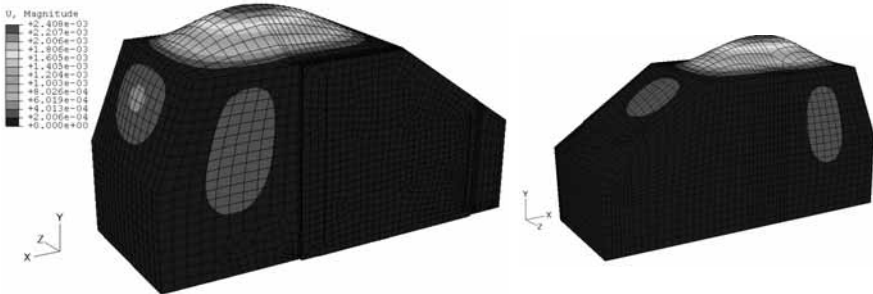


Figure 4: Predicted peak resultant displacement field of vehicle at 124.7 Hz

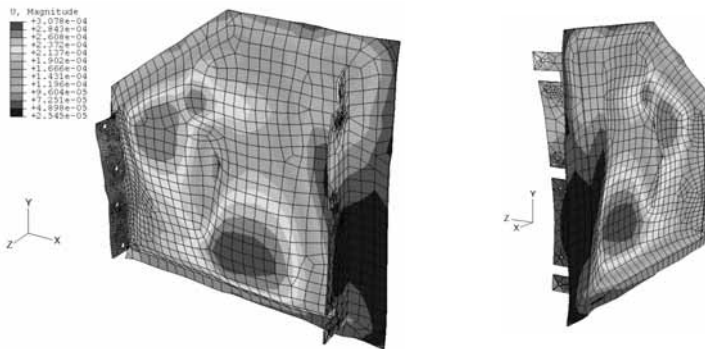


Figure 5: Predicted peak resultant displacement field of door panel at 199.38 Hz

## 8. DISCUSSION

The most important findings of the study are highlighted below:

- The study revealed that for complicated systems, such as the one under investigation, the use of residual modes only does not guarantee adequate representation of modal masses in all directions and that they should, therefore, be used in conjunction with approximately 100 eigenmodes. A combination of residual modes and higher modes seems to be the best compromise between accuracy and computational cost.
- Frequency shifts of the resonance peaks could be attributed to the effects of mass-loading of the shaker table due to the large surface areas involved.
- Based on Fig. 3, it is evident that reasonable agreement between the predicted and measured response has been attained for such sensitive measurements.
- Considering the complex nature of the environment modelled, it was observed that the simulation results predicted the general trend of the experimental data; however, as expected, small fluctuations within the experimental response were not predicted.
- Deviations between predicted and measured data may be attributed to the difficulty of accurately quantifying damping in practice, neglecting stiffness residues or by the fact that the finite element method itself is an approximate technique.

## 9. CONCLUDING REMARKS

A computational procedure for predicting door panel vibration in terms of its door mount system has been proposed and demonstrated using the finite element method. The numerical model was successfully validated by actual measurements and is amenable to giving reliable information about the vibration amplitude at any point of interest. Furthermore, the procedure may be used with confidence to formulate and identify new strategies for door mount design, selection and optimisation. Such information has proved to be worthwhile in backing up a NVH (Noise, Vibration and Harshness) reduction strategy in automotive transportation vehicles.

## 10. ACKNOWLEDGMENTS

The work described in this paper has been supported and funded by the Tshwane University of Technology, South Africa and Ford Motor Co, South Africa. The authors are grateful to Professor S Marburg of the Technical University of Mommensenstrasse, Germany and V H Balden of the University of Cape Town, South Africa for assistance in the development of the model described in this paper.

## 11. REFERENCES

- Allemang, RJ and Brown, DL. 1996. Experimental modal analysis. In: Harris, CM. Shock and vibration handbook. USA: McGraw Hill.
- Cook, RD. 1995. Finite element modelling for stress analysis. Canada: John Wiley and Sons, Inc.
- Desmet, W and Sas, P. 1996. The effect of sound adsorbing materials, plate stiffeners and vibration isolators on the vibro-acoustic behaviour of finite double wall structures. In: Sas, P (ed.). Proceedings of ISMA21, 1996, International Conference on Noise and Vibration Engineering, Vol. 1, Katholieke Universiteit, Leuven, Belgium. PMA: 101-123.
- Inman, DJ. 1994. Engineering vibration. USA: Prentice Hall, Inc.
- Irato, G, Ruspa, G and Tarzia, A. 1995 Noise quality of transient sounds: An application to the noise emitted by push-push buttons on the control panel of a car. Inter-noise 1995, S.I.: s.n.: 943-946.
- Lim, TC. 2000. Automotive panel noise contribution modelling based on finite element and measured structural-acoustic spectra. Applied Acoustics, 60: 505-519.
- Marburg, S. 2004. A survey of applications in structural-acoustic optimisation for passive noise control with a focus on optimal shell contour. Photostat copy.
- Morman, KN. 1998 Recent applications of ABAQUS to the analysis of automotive rubber components. In: 1998 ABAQUS User's Conference. Milan, Italy: Abaqus, Inc.: 23-67.
- Morrey, D and Barr, M. 1996. Optimising the dynamic response of automotive body panels. In: Sas, P (ed.). Proceedings of ISMA21, 1996, International Conference on Noise and Vibration Engineering, Vol. 3, Katholieke Universiteit, Leuven, Belgium. PMA: 1851-1862.
- Stenti, A, Moens, D and Desmet, W. 2004. Dynamic modelling of car door weather seals: a first outline. In: Sas, P and De Munck, M. (eds). Proceedings of ISMA, 2004, International Conference on Noise and Vibration Engineering, Vol. 3, Katholieke Universiteit, Leuven, Belgium. KU Leuven: 1249-1262.
- Wagner, DA, Morman, KN, Gur, Y and Koka, MR. 1997. Non-linear analysis of automotive door weatherstrip seals. Finite Elements in Analysis and Design, 28: 33-40.

Wriggers, P, Vu van T. and Stein, E. 1990. Finite element formulation of larger deformation impact-contact problems with friction. *Computers and Structures*, 37: 319-331.

Zhang, C and Brown, DL. 1996. Interior noise investigation of a passenger car by means of a mixed vibro-acoustics modal analysis. In: Sas, P (ed.). *Proceedings of ISMA21, 1996, International Conference on Noise and Vibration Engineering*, Vol. 2, Katholieke Universiteit, Leuven, Belgium. PMA: 551-563.

Zienkiewicz, OC and Taylor, RL. 2000 *The finite element method*. Vol.1, 5th ed. Oxford: Butterworth-Heinemann.